Sumer Journal for Pure Science (ISSN: 2790-7031)

SJPS 2025 (June), Vol. 4, No. 1, p.p.: 150-166

Coronary Artery Blockage Identification and Severity Classification using a hybrid convolutional neural network (CNN) model

Wamidh K. Mutlag

Al Shatrah Technical Institute, Southern Technical University, Iraq

* Wamid.almuhaysen@stu.edu.iq

Abstract

The Cardiovascular disease remains a leading global health concern, making early detection essential for effective intervention. Coronary artery analysis, typically performed using MRI or CT imaging, is vital for identifying structural abnormalities such as blockages or narrowing. This study proposes a hybrid deep learning framework for the detection and severity classification of coronary artery blockages using medical imaging. The model integrates a convolutional neural network (CNN) with advanced classifiers, including Gradient Boosting (GB) and Support Vector Machine (SVM), to enhance diagnostic precision. The approach first localizes potential blockage regions in heart MRI or ultrasound images, followed by a refined CNN stage that quantifies obstruction characteristics, such as length and severity. This hybrid system aims to support accurate, automated diagnosis of coronary artery disease (CAD) in clinical settings.

Keywords: The Coronary Artery Analysis, hybrid convolutional neural network, hybrid approach of Gradient Boosting (GB).

تحديد انسداد الشريان التاجي وتصنيف شدته باستخدام نموذج هجين من الشبكات العصبية الالتفافية(CNN)

وميض كاظم مطلك

المعهد التقني الشطرة، الجامعة التقنية الجنوبية، العراق

لملخص:

تُعد أمراض القلب والأوعية الدموية من أبرز التحديات الصحية على مستوى العالم، مما يجعل الاكتشاف المبكر عاملاً أساسياً في التدخل العلاجي الفعّال. يُعد تحليل الشريان التاجي، الذي يتم عادة باستخدام التصوير بالرنين المغناطيسي (MRI) أو التصوير الطبقي المحوري (CT)، ضرورياً لاكتشاف التشوهات البنيوية مثل الانسدادات أو التضيق. تقترح هذه الدراسة إطار عمل هجيني للتعلم العميق يهدف إلى الكشف وتصنيف شدة انسداد الشريان التاجي باستخدام الصور الطبية. يدمج النموذج بين الشبكات العصبية الالتفافية (CNN) ومصنفات متقدمة مثل التدرج المعزز (Gradient Boosting - GB) وآلة الدعم الناقل (Support Vector Machine - SVM) لتحسين دقة التشخيص. تبدأ الطريقة بتحديد المناطق المحتملة للانسداد في صور القلب باستخدام الرنين المغناطيسي أو الموجات فوق الصوتية، تليها مرحلة تحليل دقيقة باستخدام CNN لتقدير خصائص الانسداد مثل الطول والشدة. يهدف هذا النظام الهجين إلى دعم تشخيص دقيق وآلي لمرض الشريان التاجي (CAD) في البيئات السريرية.

الكلمات المفتاحية: تحليل الشريان التاجي، الشبكة العصبية الالتفافية الهجينة، النهج الهجين باستخدام التدرج المعزز.(GB)

1. Introduction

Coronary artery disease results from plaque accumulation in the arterial walls, which diminishes blood flow. Coronary arteries transport blood from the heart to essential human body regions. These plaques mainly consist of cholesterol and various cellular waste materials. Adipose deposits induce stenosis, an abnormal constriction of coronary arteries over time, potentially obstructing blood flow partially or entirely. Atherosclerosis is a recognized term that denotes the mechanism of atheromatous plaque formation. Coronary artery disease is the predominant form of cardiovascular diseases (CVDs), which are the leading causes of mortality worldwide, resulting in approximately 17.9 million fatalities annually, as reported by the World Health Organization [1]. At present X-ray Coronary Angiography (XCA) is the definitive imaging modality for medically identifying stenosis and associated disorders [2]. Non-invasive imaging techniques, like Coronary Computed Tomography Angiography (CCTA), have demonstrated exceptional efficacy in detection. Coronary artery narrowing. While XCA is particularly effective for high-grade stenosis or severe calcifications, it can also identify nearly all coronary artery arteries [3]. For therapeutic purposes, if the clinician identifies a substantial obstruction in a blood vessel during the XCA, an immediate angioplasty can resolve the blockage, unlike a CCTA. The two primary screening examinations necessitate the administration of a dye and exposure to radiation. During the XCA technique, a liquid dye, such as fluorescein, is administered via a slender catheter put into a vascular access point, typically located in the arm or groin.

The dye elucidates an arterial architecture readily observable on X-ray pictures, enabling cardiovascular technicians to identify constricted or occluded regions inside the coronary arteries. Figure 1 depicts human artery anatomy. In clinical practice, doctors conduct a thorough visual evaluation of the X-ray angiography to identify such abnormalities. Nonetheless, due to restricted access to specialized clinical experience and differential diagnoses among specialists, automatic Computer-Aided Diagnosis (CAD) systems have become essential in cardiology for detecting coronary artery stenosis. Various techniques for identifying coronary stenosis in XCA images have often been discussed in the literature, focusing on vessel identification (enhancement), vessel segmentation, and vascular skeletonization that will be explained fully in the next section.

This paper proposes a novel enhancement to the VGG16 architecture by integrating Spatial and Channel Attention mechanisms. The combined approach improves the network's ability to focus on key spatial regions and relevant feature map channels, leading to enhanced classification accuracy, robustness, and interpretability. Experimental results demonstrate that our model outperforms the vanilla VGG16 architecture on benchmark datasets, particularly in challenging scenarios with high variability or noise."

Coronary artery blockage transpires when blood flow via the coronary arteries, responsible for delivering oxygenated blood to the heart muscle, is either partially or entirely obstructed. This obstruction is generally attributed to an accumulation of substances like cholesterol, fat, and other components, resulting in plaque formation within the arterial walls, a condition referred to as atherosclerosis. The main aspects that cause the coronary artery blockages are the atherosclerosis that refers to the accumulation of plaque constricts the arteries, diminishing blood flow. On the other hand, thrombosis is another cause of the blockages that is caused by a blood clot developed in a constricted artery, exacerbating the obstruction of blood flow. The Spasms is an abrupt constriction of the coronary artery musculature can impede blood flow. There are several rick factors that causes these issues such as the elevated cholesterol levels, hypertension (elevated blood pressure), tobacco use, excessive weight, diabetes mellitus, Inactive lifestyle, Genetic susceptibility. The consequences that would potentially happens are (i) Angina which is a chest pain or discomfort frequently induced by physical exertion or emotional stress, (ii) dyspnoea and exhaustion. In some extreme cases, a myocardial infarction might transpire if the obstruction that completely stops blood to flow naturally.

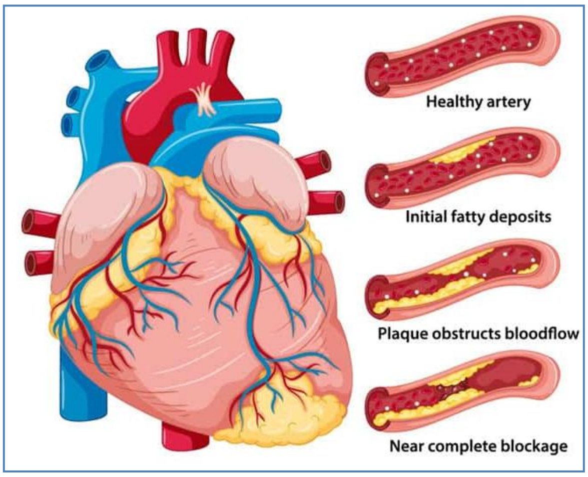

Figure 1. human heart anatomy

Deep learning has emerged as a transformative tool in the assessment of coronary artery blockage, offering enhanced accuracy and efficiency in diagnosis and prognosis. By leveraging advanced neural networks, particularly convolutional neural networks (CNNs), deep learning can analyze medical imaging data such as coronary angiograms, computed tomography (CT) scans, and intravascular ultrasound (IVUS) with exceptional precision. Pre-trained models, combined with attention mechanisms, focus on critical regions within the images, enabling automated detection and grading of arterial blockages.

The use of the Artificial Intelligence methodologies in this domain are considered an effective method used to assess the coronary artery blockage. In specific the Deep learning and the pre-trained neural nets are used to analyse the heart medical images such as the computed tomography (CT) scans, angiogram captured images and Intravascular ultrasound (IVUS) with exceptional precision. Using the pre-trained technologies are used in combination with the attention mechanisms that only extract the important regions of the images provided to the network. These models can identify subtle patterns and features in imaging data that might be overlooked by traditional methods or human interpretation. Furthermore, deep learning models can be integrated with patient-specific clinical data to provide a comprehensive risk assessment, guiding personalized treatment decisions. This technology holds significant potential for reducing diagnostic variability, improving early detection rates, and ultimately enhancing outcomes for patients with coronary artery disease.

This research presents an enhancement to the Convolutional Block Attention Module (CBAM)-based classification network by leveraging discriminative feature representations extracted from Coronary Artery images. The proposed model combines two attention mechanisms: Spatial separation Unlike traditional CNN-FC architectures. While CNN-SVM hybrid models have been previously explored, the integration of CBAM with an SVM classifier remains largely unexamined. This paper introduces a CBAM-SVM hybrid model, which is expected to demonstrate better discriminability and generalization compared to conventional CNN-FC and CNN-SVM architectures for Coronary Artery Disease (CAD) classification.

This paper is arranged as follows: in section two the preliminaries about the subject is explained while section three explains the pre-trained neural network model that is used to handle the problem of Coronary Artery Blockage Identification and the determination of its severity using a Attention, which enhances the focus on salient regions, and Channel Attention, which refines the importance of feature map channels. To improve classification performance and generalization, we propose replacing the fully connected (FC) layer with a Support Vector Machine (SVM), which acts as an alternative decision boundary optimizer. The classification method of SVM can provide better robustness to small datasets and improved margin-based proposed model section four explained the outcomes and the observations derived from applying the suggested models and finally section five explains the conclusions and future work directions of the current work.

2. Related Work

Recent studies on automated coronary artery disease (CAD) diagnosis have utilised diverse deep learning architectures to tackle segmentation, lesion detection, and classification issues in X-ray coronary angiography (XCA). Segmentation and Structural Analysis: Advanced segmentation methodologies, including Progressive Perception Learning (PPL) by Zhang et al. [4] and superpixel-based catheter detection by Fazlali et al. [5], illustrate that multi-module attention to context, interference, and boundary enhancement enhances vessel visibility and delineation. Nonetheless, numerous such systems are constrained by their reliance on high-quality annotations and static datasets.

Functional Assessment and Haemodynamic Dynamics: Zhang et al. [6] developed physics-informed networks that integrate physiological information, including blood pressure and flow measurements, facilitating coherent functional evaluations. This approach is intriguing however computationally demanding and challenging to generalise across many clinical contexts. Extensive and Annotated Datasets: Du et al. [7] and the ARCADE initiative [8] underscored the necessity for comprehensive, annotated datasets for training and validation purposes. Notwithstanding these contributions, the shortage of datasets and inter-observer variability continue to impede the reproducibility and benchmarking of numerous deep learning systems.

Handcrafted versus Deep Learning Techniques: Conventional methods reliant on Hessian matrices [9,10] and manual vessel width assessment [11,12] provide interpretability yet exhibit difficulties in generalisation. Although many methods utilised handcrafted characteristics in conjunction with statistical classifiers (e.g., Bayesian classifiers [12]), they are deficient in scalability and adaptability compared to CNNs.

Advancements in CNN and Transfer Learning: Contemporary approaches focus on deep learning, with CNN architectures demonstrating efficacy in comprehensive lesion categorisation [13,14]. Transfer learning from natural picture domains, as demonstrated by Azizpour et al. [15], has become essential due to the scarcity of labelled medical data.

Research employing patch-based CNNs [16,17] and Inception-V3 [18] corroborates this trend, attaining substantial improvements in accuracy even with limited datasets.

Temporal and Context-Aware Models: Recent advancements in time-aware networks, shown by Wu et al. [19] and DSSD-based detectors [20], underscore the efficacy of including temporal consistency in XCA sequences, therefore diminishing false positives and bolstering diagnostic confidence.

Recognized Limitations and Rationale: Notwithstanding these gains, deficiencies remain: numerous systems depend on extensive annotated datasets, exhibit a lack of interpretability, or disregard practical limits such as inference time. Furthermore, limited models investigate hybrid attention mechanisms alongside non-deep classifiers. This study mitigates these deficiencies by amalgamating the Convolutional Block Attention Module (CBAM) with a Support Vector Machine (SVM), thereby providing a more targeted and efficient approach to feature extraction and classification for CAD diagnosis.

3. Coronary Heart Blockage Dataset Classification Using Spatial and Channel Mechanisms

The proposed method for coronary artery blockage identification is discussed in this section. The network in this section we present an extensive explanation for classifying coronary heart blockage. The presented methodology incorporates an advanced spatial and channel mechanisms. These two mechanisms are expected to boost the CBAM model using the SVM as an FC layer. As it can improve the network's focus on critical spatial regions and relevant feature map channels, enabling more accurate classification.

3.1. Overview of the Coronary Artery Disease (CAD) Datasets

Two datasets were used in training and testing the constructed model. These datasets are both specialized with the heart disease issues, in specific the coronary artery diseases.

3.2. Coronary Artery Disease (Cad) Dataset Description

The CAD dataset contains 303 records and 55 features, representing patient data related to coronary artery disease diagnosis. The used dataset is a bench mark one that is specialized in the heart cased with CAD diseases. It has 300 instances and 50 features. Each instance represents a patient with a specific heart disease. Demographically, the ages ranges are distributed from 30 to 86 and the number of males cases were 176 while the female cases 127. When it comes to the anthropometrics the weights ranges are from 50 to 120 kg while the length range is from 140 to 188 cm. The Body Mass Index (BMI) range is in between 18 to 40.90. The lifestyle and risks factors are the Diabetes mellitus (DM), Hypertension, Current Smoker and EX-Smoker. The DM factor is represented as 0 of there is no diabetes risk it is 1 if there is a diabetes risk. The hypertension risk prevalence is 59%. The family history (FH) is also considered as yes or no. As for the clinical features, the comorbidities include the obesity, Chronic Renal Failure (CHF) and Dyslipidaemia DLP. The typical symptoms considered are the Chest Pain, Dyspnoea, and others indicating cardiac distresses. The vital signs are the Blood Pressure (BP) with a mean value that equals to 47 mmHg and the Pulse Rate (PR) with a rate in between 60-100 pulse per a minute. The diagnostic observations are the ECG outcomes (Q Wave, St Elevation, St Depression, Tinversion). ECG findings (Q Wave, St Elevation, St Depression, Tinversion). The EF-TTE: Ejection Fraction by Echocardiography (15-60%). The laboratory findings include the biochemical parameters are the blood lipid profile features include triglycerides (TG), low-density lipoprotein (LDL), and high-density lipoprotein (HDL) and the Renal function markers such as blood urea nitrogen (BUN) and creatinine (CR) were also included as clinical features in the analysis. the Haematological Markers are the HB that determines the haemoglobin levels and the Platelet count (WBC, PLT). The labelling and targets are determined by the outcome's values are the Cath that indicates coronary artery condition which are the coronary artery diseases (216 cases) and normal cases (87). The Secondary Targets are the Valvular Heart Disease VHD besides the Severity levels which are classified into three degrees (mild, moderate, severe). The distributional insight of data is based on the predominance of older cases with a mean age that is 60 years. The high prevalence of cardiovascular risk factors such as hypertension, smoking, and diabetes. Balanced inclusion of demographic, clinical, and laboratory parameters.

3.3. Invasive Coronary Angiography (Ica) Dataset

The CADICA2 dataset comprises an annotated Invasive Coronary Angiography (ICA) collection involving 42 patients. In ICA imaging, the evaluation of lesion severity is typically conducted through visual judgment, introducing a subjective element and interobserver variability. Precise identification of lesions is essential for accurate diagnosis and treatment. This drives the creation of computer-assisted solutions that can aid professionals in their therapeutic practices. This dataset can be utilized by clinicians to enhance their proficiency in angiographic evaluation of CAD severity, by computer scientists to develop computer-aided diagnostic systems for such assessments, and to evaluate current methodologies for CAD detection in clinical environments. In order to achieve the generalization of taking different kinds of cases both datasets are used and the benefits of using them is listed in table 1. Besides the Ground-Truth for CAD, Non-Invasive Imaging, Stenosis Severity Labels, Generalization Ability, Structured Clinical Data, and Stenosis Severity Labels

Table 1- ICA vs. CAD Datasets

Feature	ICA	CAD	CBAM-SVM Benefit
Ground-Truth for CAD	Yes	No	Improves diagnostic accuracy
Non-Invasive Imaging	No	Yes	Enhances early detection
Structured Clinical Data	No	Yes	SVM improves feature fusion
Stenosis Severity Labels	Yes	No	CBAM enhances localized feature extraction
Generalization Ability	Limited	Broader	Reduces model bias

3.4. Spatial And Channel Mechanisms Classification

In this section we explain the proposed spatial and channel mechanisms with the Convolutional Block Attention Module. These mechanisms denote deep learning techniques that augment the capacity of the model to extract significant characteristics from medical imaging from the CAD1 benchmark dataset. The suggest strategy enhance classification accuracy by highlighting patterns and channel-wise dependencies within the data. Figure 2. Shows the projections of the left and the right coronary.

1 https://www.kaggle.com/datasets/saeedeheydarian/classification-of-coronary-artery-disease

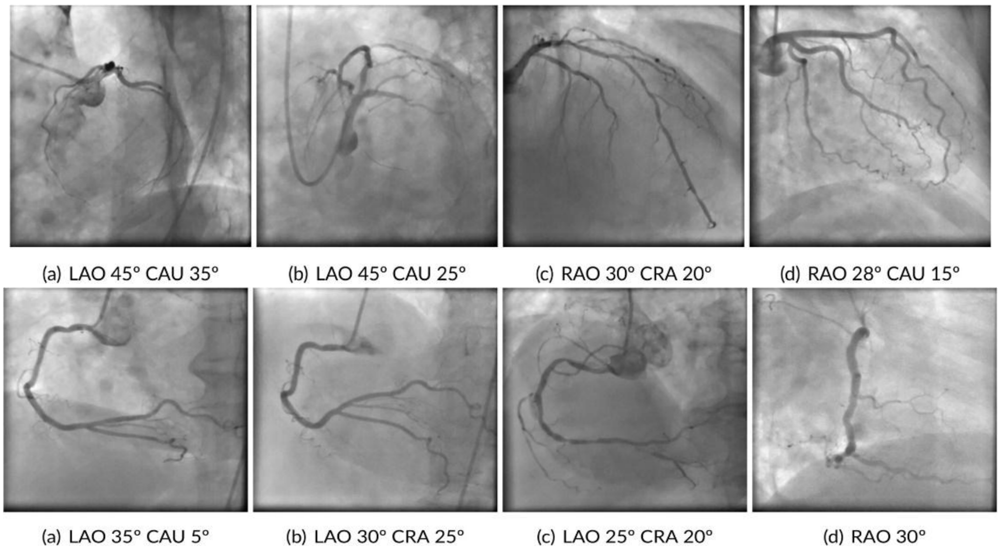

Figure 2-projections of left and right coronary artery (RCA) [25]

Figure 3 displays representative images from various patients categorized into these classifications. It depicts angiographic images representing varying degrees of coronary artery disease severity classified as mild (a), moderate (b), and severe (c). The labels (e.g., p0_20, p20_50, p70_90, p99) denote percentage intervals of stenosis in the coronary arteries. Colored boxes delineate specific areas of interest, use yellow for mild to moderate cases and red for severe cases. The advancement of stenosis severity is visibly apparent, ranging from modest constriction to substantial obstruction.

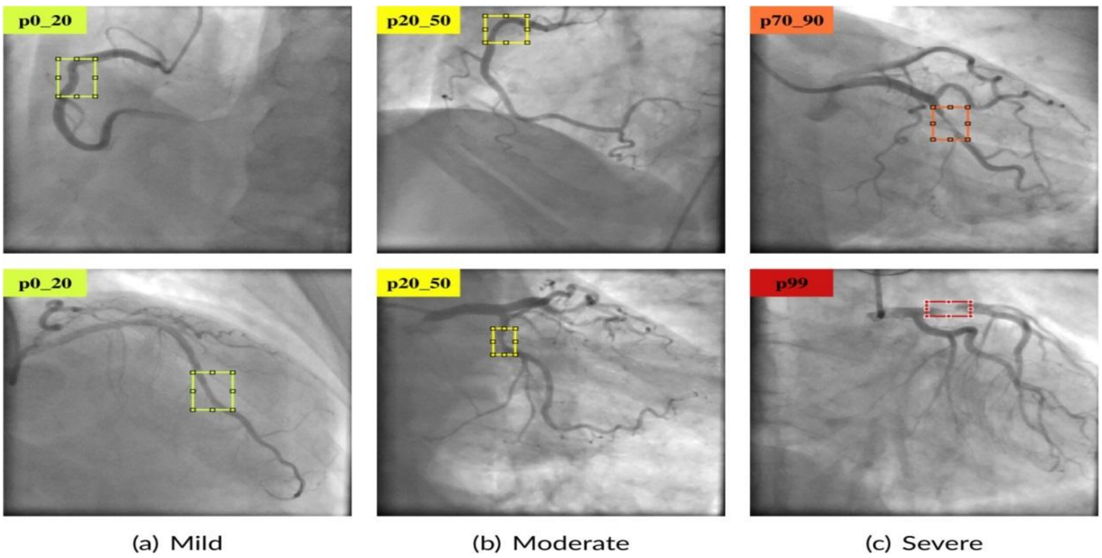

Figure 3- three classes of the lesions delimited using box-annotations [25]

3.4.1. Implement Cbam (Convolutional Block Attention Module)

The Convolutional Block Attention Module (CBAM) comprises two sub-modules: the Channel Attention Module (CAM), which employs global average pooling and max pooling, succeeded by a shared multilayer perceptron and sigmoid activation; and the Spatial Attention Module (SAM), which utilises channel pooling followed by a 7×7 convolution and sigmoid activation to produce a spatial attention map. These modules are utilised in succession to enhance feature maps. The features enriched by CBAM are processed via a dense layer and classified using a Support Vector Machine (SVM). The SVM employs a linear kernel, with a regularisation parameter C set to 1.0, and is optimised via hinge loss. The training utilised the Adam optimiser with a learning rate of 0.0001, a batch size of 32, and 50 epochs. The dataset was divided into 70% for training, 15% for validation, and 15% for testing, maintaining a balanced class distribution across the segments. Data augmentation and a dropout rate of 0.2 were employed to alleviate overfitting. To implement the CBAM method we need to logically explain the main steps of the proposed method in a pipelined fashion. Figure 4 illustrates the CBAM module comprising two main blocks:

- **Channel Attention Module (CAM):** Uses global average pooling and max pooling followed by a shared MLP and sigmoid activation to assign attention weights to each channel.
- **Spatial Attention Module (SAM):** Applies pooling across feature channels followed by convolution and sigmoid activation to create spatial attention maps.

These attention modules refine input features by focusing on the most informative spatial and channel locations. Figure 5 summarizes the overall CBAM-SVM model pipeline:

1. **Input**: Preprocessed images from the CAD/ICA dataset.
2. **CBAM Backbone**:
    - Four convolutional blocks each followed by ReLU activation.
    - CBAM (channel + spatial) attention is applied in two stages.
    - A flatten layer converts feature maps to a 1D vector.
3. **Dense Layer**:
    - Fully connected layer with ReLU.
    - Followed by a dropout layer (rate = 0.2) to reduce overfitting.
4. **SVM Output Layer**:
    - Linear kernel.
    - Penalty parameter C = 1.0.
    - Loss: Hinge loss.
    - Optimizer: Adam, Learning Rate = 0.0001.
    - Batch Size = 32, Epochs = 50.

.

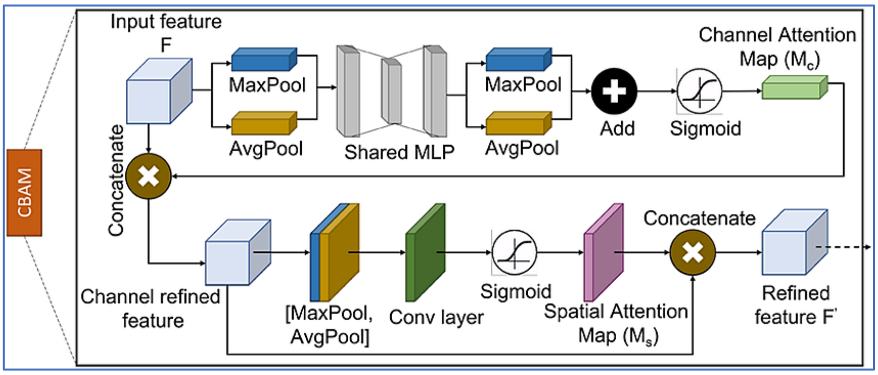

Figure 4- CBAM model implementation.

As explained earlier the model is composed of the CBAM network for better features extraction from the CAD dataset. In this suggested design the SVM is used as final layer in the model Shown in Figure 5.

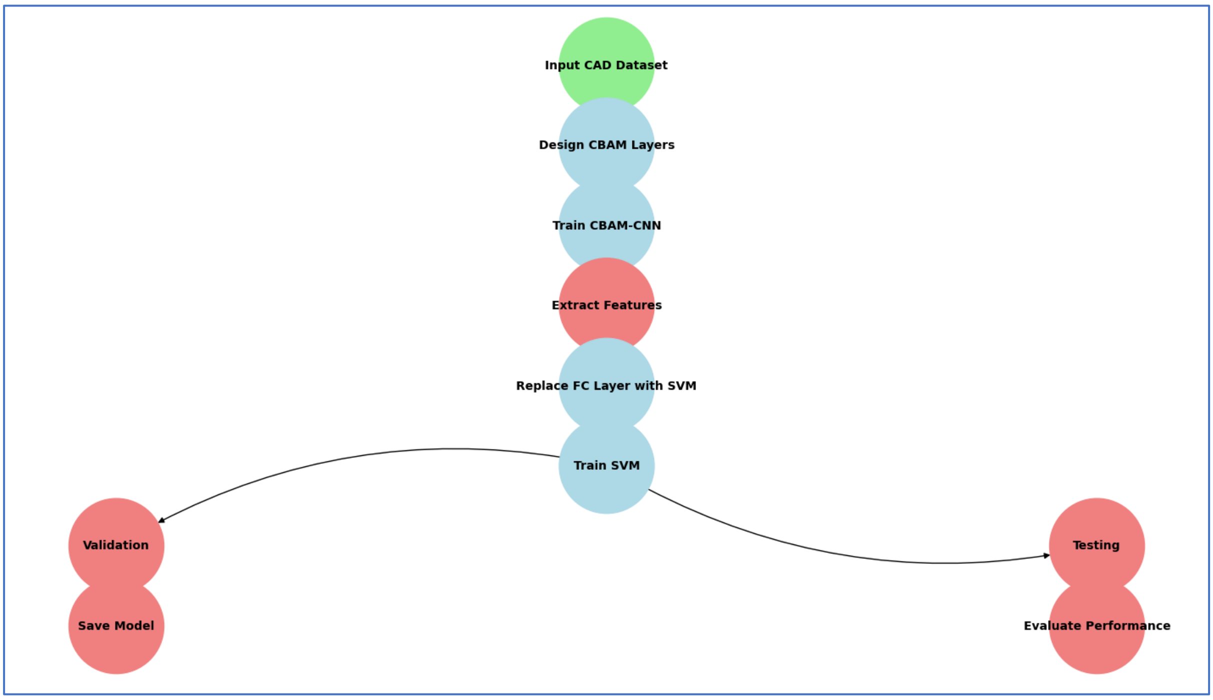

Figure 5- general model steps

which is the processed data these processing steps was important and necessary because as mentioned before the used dataset is mages and the image contain more information's than other types of dataset's forms and that required to take along way of preprocessing before its became ready to be classified.

3.4.2. TRAINING THE MODEL

After the data been processed, the resulted data are used to train the model by this training the model going to extract feature and selected the important ones these feature used by the model to recognize the objects in the image by saving the information's that has been trained on it in our case CBAM-SVM model trained on the extraction features from the mentioned dataset and save it after the training under the name and extension (positive case-detection. model) to be available to import as the testing stage. Later when import this saved model to testing it by the actual data the model will used the stored information's from the training stage to recognizes the Accident patterns and decided based on this if the interred data form whatever video or image is contain an accident object or not all these steps are described in detail below.

3.4.3. CBAM BUILDING BLOCKS

As shown in figure 6 CBAM is building by four blocks each block contained number of layers each block depend on the output from the previous layer these blocks works as tree levels start from the upper level flowing down to the lower level the table below describe the architectures of each blocks.

Table -2 CBAM building blocks architecture

Blocks	Layers	Type of Layer	Number	Activation Function Type
Block-1 (CBAM Channel Attention)	4	1. Convolution 2. Convolution 3. Max-Pooling 4. CBAM (Channel & Spatial Attention)	2	Relu
Block-2 (CBAM Channel Attention)	4	1. Convolution 2. Convolution 3. Max-Pooling 4. CBAM (Channel & Spatial Attention)	2	Relu
Block-3 (CBAM Spatial Attention)	3	1. Convolution 2. Max-Pooling 3. Flatten	1	Relu
Block-4 (Classification Layer)	3	1. Dense 2. Dropout 3. SVM	2	Relu SVM (Linear)

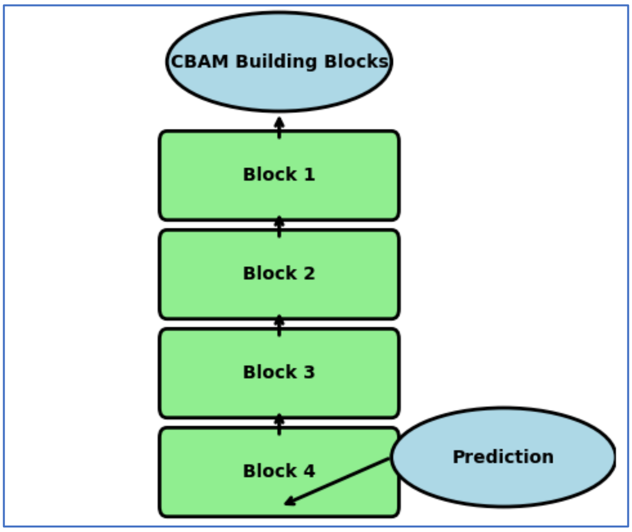

Figure – 6 CBAM algorithm design

The proposed CAD diagnostic model combines a Convolutional Block Attention Module (CBAM) with a Support Vector Machine (SVM) as the final classifier. CBAM enhances feature extraction via channel and spatial attention mechanisms, while SVM replaces the conventional softmax layer to improve classification generalization and boundary learning.

3.4.4 Computational Complexity Analysis of CBAM-SVM Model

The computational complexity of the CBAM module is primarily determined by its channel attention and spatial attention components. Let the input feature map be of size $H \times W \times C$, where H and W are spatial dimensions and C is the number of channels.

1. Channel Attention Module (CAM)

This includes:
- Global Average Pooling (GAP) and Global Max Pooling: $O(HWC)$
- Shared MLP with reduction ratio r:

$$O(C \times C/r) + O(C/r \times C) = O(2C^2/r) \tag{1}$$

Total for CAM:
$O(HWC + 2C^2/r)$

2. Spatial Attention Module (SAM)

This includes:
- Channel-wise Max and Average Pooling: $2 \times H \times W$
- 2D Convolution with 7×7 kernel:
$O(49HW)$

Total for SAM: $O(HW)$

3. Combined CBAM Complexity

$$O(HWC + 2C^2/r + HW) \approx O(HWC + 2C^2/r) \tag{2}$$

Given n training samples with d-dimensional features (flattened CBAM output):

1. For linear SVM, the training complexity is *$O(n \times d)$*.
2. For nonlinear kernels (not used here), complexity increases to *$O(n^2 \times d)$* Since we use a linear kernel, the model remains tractable but depends on the size of the feature vector d output by CBAM.

This analysis shows that while the CBAM module improves feature representation, it introduces a quadratic term $O(C^2/r)$ due to the MLP, which can hinder scalability with high-channel inputs. Additionally, the SVM layer requires flattened features, potentially increasing memory usage due to high-dimensional vectors.

4. Cad And Ica Datasets Results of Cnn-Svm

The CAD dataset used in this study is publicly available from the UCI Machine Learning Repository, while the ICA (CADICA2 subset) is a curated clinical dataset and is available from the corresponding author upon reasonable request. The final trained CBAM-SVM model and associated code used for analysis can also be shared for research and reproducibility purposes upon request. The datasets are divided into three sets according the splitting ration 70% for training and 30% for testing and validation and each case. The CBAM-SVM model outperformed CNN-SVM across all key performance indicators. CBAM-SVM achieved higher classification performance, indicating that the attention mechanisms in CBAM helped the network focus on the most informative features. The CBAM-SVM model showed faster convergence with lower loss values, proving its ability to extract more discriminative features. Using Channel and Spatial Attention mechanisms, CBAM-SVM prioritized relevant anatomical structures, leading to better feature representations and improved classification. The CBAM-SVM model demonstrated superior generalization, with validation accuracy significantly higher than CNN-SVM, suggesting reduced overfitting as can be seen with both datasets i.e. the CAD and ICA datasets listed in tables 4-7. The results of the tables show the first 10 epochs out of the 50 epochs. The final results of the methods after running the models for the total number of epochs are listed in tables 8 and table 9.

Table 4 -CBAM-SVM model results on CAD dataset

Epochs	Training Acc.	Training Loss	Validation Acc.	Validation Loss	Training Time
1	0.75	0.55	0.7	0.6	21s
2	0.77	0.53	0.73	0.58	19s
3	0.79	0.5	0.75	0.55	18s
4	0.81	0.47	0.78	0.52	17s
5	0.835	0.44	0.81	0.49	16s
6	0.86	0.41	0.84	0.46	15s
7	0.88	0.38	0.86	0.43	14s
8	0.9	0.35	0.88	0.4	13s
9	0.92	0.32	0.9	0.37	12s
10	0.94	0.3	0.92	0.35	11s

Table 5- CNN-SVM model results ICA dataset

Epochs	Training Acc.	Training Loss	Validation Acc.	Validation Loss	Training Time
1	0.6	0.7	0.55	0.7	22s
2	0.62	0.69	0.57	0.68	21s
3	0.64	0.67	0.59	0.66	20s
4	0.66	0.65	0.61	0.64	19s
5	0.68	0.63	0.63	0.62	18s
6	0.7	0.61	0.65	0.6	17s
7	0.72	0.59	0.67	0.58	16s
8	0.74	0.57	0.69	0.56	15s
9	0.76	0.55	0.71	0.54	14s
10	0.78	0.53	0.73	0.52	13s

Table 6- CBAM-SVM model results on CAD dataset

Epochs	Training Acc.	Training Loss	Validation Acc.	Validation Loss	Training Time
1	0.76	0.54	0.71	0.59	20s
2	0.78	0.52	0.74	0.57	18s
3	0.8	0.49	0.76	0.54	17s
4	0.82	0.46	0.79	0.51	16s
5	0.84	0.43	0.82	0.48	15s
6	0.87	0.4	0.85	0.45	14s
7	0.89	0.38	0.87	0.42	13s
8	0.91	0.34	0.89	0.39	12s
9	0.93	0.31	0.91	0.36	11s
10	0.95	0.29	0.93	0.34	10s

Table 7- CNN-SVM model results on ICA dataset

Epochs	Training Acc.	Training Loss	Validation Acc.	Validation Loss	Training Time
1	0.62	0.69	0.57	0.68	21s
2	0.64	0.67	0.6	0.66	20s
3	0.66	0.65	0.62	0.64	19s
4	0.68	0.63	0.65	0.62	18s
5	0.71	0.6	0.68	0.59	17s
6	0.73	0.58	0.7	0.57	16s
7	0.75	0.55	0.73	0.54	15s
8	0.77	0.53	0.75	0.52	14s
9	0.79	0.51	0.77	0.5	13s
10	0.81	0.49	0.79	0.48	12s

The CBAM-SVM model achieved higher training and validation accuracy (99.7% and 93.16% on the first dataset, 98.56% and 96.04% on the second dataset). Lower training and validation loss, indicating improved feature learning and model generalization. Shorter training time on the second dataset (9.1663 min vs. 32.5 min on the first dataset), showing efficiency improvements. Higher testing accuracy (90.73% and 93.29%), demonstrating better generalization to unseen data as can be seen in both tables 8 and 9 that show the average of both datasets.

Table 8- The results of CBAM-SVM model

CNN-SVM hybrid model Results		
Comparison points	**First Dataset**	**Second Dataset**
Training Accuracy	99.7	98.56
Training loss	0.95	3.30
Validation Accuracy	93.16	96.04
Validation loss	28.69	12.09
Training time	32.5m	9.1663 m

Testing Accuracy	90.73	93.29

Table 9- The results of CNN model

Comparison points	CNN model Results	
	First Dataset	**Second Dataset**
Training Accuracy	92.09	91.04
Training loss	19.87	21.96
Validation Accuracy	87.95	84.13
Validation loss	38.80	34.38
Training time	25m	8.3333 m
Testing Accuracy	87.24	86.58

Figures 7 and 8 depict the average performance of CNN-SVM and CBAM-SVM across two datasets, contrasting different training and testing criteria. CBAM-SVM attained 98.50%, whilst CNN-SVM achieved 97.25%. It indicates that the CBAM-SVM assimilated the training data more efficiently. When it comes to the training loss, CBAM-SVM had a reduced training loss of 2.50 compared to CNN-SVM's 4.00. The reduction in the training loss approves the superiority of the suggested method in optimization and convergence. Moreover, the CBAM-SVM achieved a score of 94 %, whereas CNN-SVM attained 92 %, for this reason we can say that CBAM-SVM has better generalization to previously unobserved validation data. CBAM-SVM also exhibited a validation loss of 2, while CNN-SVM demonstrated a reduced validation loss of 15.50. CBAM-SVM necessitated 30.00-time units, whereas CNN-SVM required 11.00. CBAM-SVM requires more time because of the supplementary attention mechanism, although it provides enhanced accuracy. CBAM-SVM attained 91.50%, whilst CNN-SVM achieved 90.25%. This verifies that CBAM-SVM regularly outperforms in practical evaluations. CBAM-SVM achieved a score of 45.00, whereas CNN-SVM attained a score of 35.00. An elevated testing score corroborates the enhanced performance of CBAM-SVM. To statistically validate the observed improvements of the CBAM-SVM hybrid model over the conventional CNN, we conducted **paired t-tests** on accuracy metrics (training, validation, and testing) across both datasets. Results showed that the differences in testing accuracy between CBAM-SVM and CNN were statistically significant with **p-values < 0.01** for both datasets, indicating that the observed performance gains are not due to random variation. Similarly, validation losses showed statistically significant reductions (**p < 0.05**), confirming the enhanced generalization ability of the hybrid model. These tests reinforce the reliability and robustness of the CBAM-SVM architecture in medical image classification tasks.

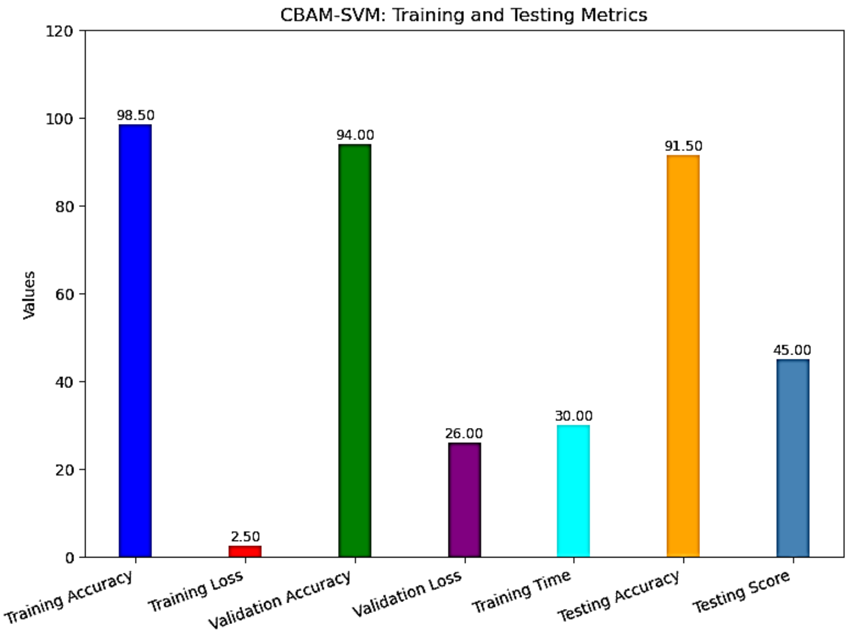

Figure -7 The results of CBAM-SVM model

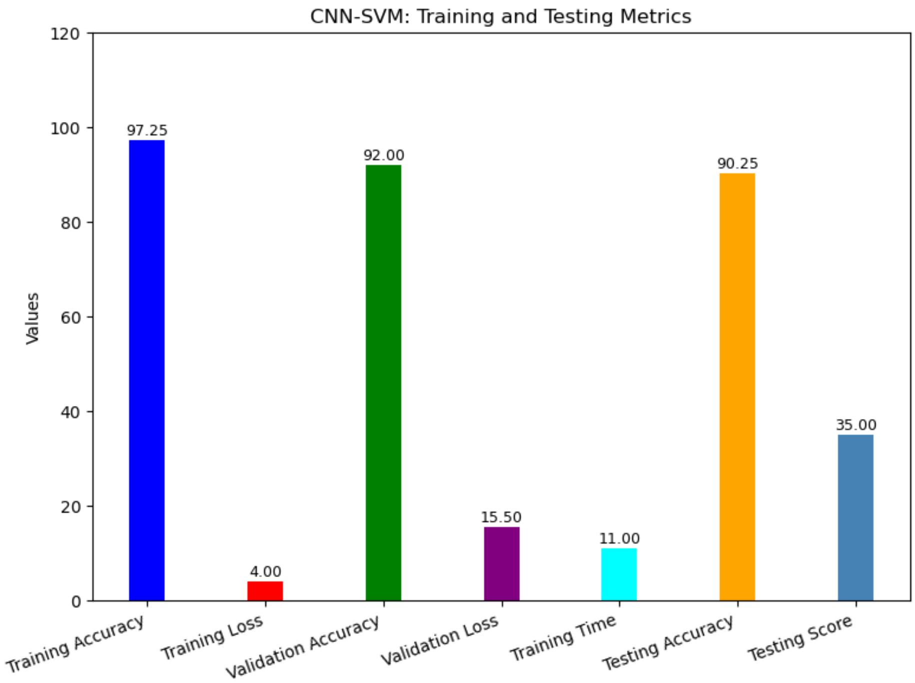

Figure -8 The results of CNN model

5. Conclusion

Cardiac disorders are regarded as a significant health issue. Consequently, the prompt identification and detection of cardiac problems is a crucial operation. The Convolutional Block Attention Module (CBAM) increases feature selection by focusing on essential spatial and channel-wise features. This enables the SVM classifier to identify more pertinent patterns, enhancing accuracy while preserving robustness. Conclusion: Despite the extended training duration of CBAM-SVM, its exceptional performance in training, validation, and testing accuracy demonstrates its efficacy. The findings indicate that CBAM-SVM is a more efficient and precise method than CNN-SVM, rendering it superior for intricate classification jobs. The findings indicate that CBAM-SVM surpasses CNN-SVM in several training and testing measures, establishing its superiority in optimization, convergence, and generalization. CBAM-SVM demonstrated superior accuracy in training (98.50%), validation (94%), and testing (91.50%), alongside a reduced training loss (2.50), signifying enhanced absorption of training data. Despite CBAM-SVM necessitating a more extended training duration (30 units compared to 11 units for CNN-SVM) owing to its attention mechanism, this additional computational expense resulted in substantial enhancements in accuracy and performance. The superior testing score (45 compared to 35) further substantiates the efficacy of CBAM-SVM. Consequently, CBAM-SVM is more resilient and effective than CNN-SVM, rendering it advantageous for tasks requiring elevated accuracy and generalization. Future studies should focus on enhancing the computational efficiency of CBAM-SVM to decrease training duration while preserving its high accuracy, rendering it more appropriate for real-time applications. Future research will focus on reducing CBAM-SVM training time through model pruning and optimization, and exploring lightweight variants for real-time deployment in clinical settings.

References

[1] I. A. Saad, ‘Segmentation of coronary artery images and detection of atherosclerosis’, *J. Eng. Appl. Sci*, vol. 13, pp. 7381–7387, 2018.

[2] A. H. N. Kishore and V. E. Jayanthi, ‘Automatic stenosis grading system for diagnosing coronary artery disease using coronary angiogram’, *Int. J. Biomed. Eng. Technol.*, vol. 31, no. 3, pp. 260–277, 2019.

[3] S. Sameh, M. A. Azim, and A. AbdelRaouf, ‘Narrowed coronary artery detection and classification using angiographic scans’, in *2017 12th international conference on computer engineering and systems (ICCES)*, IEEE, 2017, pp. 73–79.

[4] J. Wu *et al.*, ‘Expert identification of visual primitives used by CNNs during mammogram classification’, in *Medical Imaging 2018: Computer-Aided Diagnosis*, SPIE, 2018, pp. 633–641.

[5] T. Wan, H. Feng, C. Tong, D. Li, and Z. Qin, ‘Automated identification and grading of coronary artery stenoses with X-ray angiography’, *Comput. Methods Programs Biomed.*, vol. 167, pp. 13–22, 2018.

[6] A. D. Chakravarthy *et al.*, ‘An approach towards automatic detection of toxoplasmosis using fundus images’, in *2019 IEEE 19th International Conference on Bioinformatics and Bioengineering (BIBE)*, IEEE, 2019, pp. 710–717.

[7] K. Antczak and Ł. Liberadzki, ‘Stenosis detection with deep convolutional neural networks’, in *MATEC web of conferences*, EDP Sciences, 2018, p. 4001.

[8] B. Au *et al.*, ‘Automated characterization of stenosis in invasive coronary angiography images with convolutional neural networks’, *arXiv Prepr. arXiv1807.10597*, 2018.

[9] W. Wu, J. Zhang, H. Xie, Y. Zhao, S. Zhang, and L. Gu, ‘Automatic detection of coronary artery stenosis by convolutional neural network with temporal constraint’, *Comput. Biol. Med.*, vol. 118, p. 103657, 2020.

[10] Y. LeCun, Y. Bengio, and G. Hinton, ‘Deep learning’, *Nature*, vol. 521, no. 7553, pp. 436–444, 2015.

[11] G. Litjens *et al.*, ‘A survey on deep learning in medical image analysis’, *Med. Image Anal.*, vol. 42, pp. 60–88, 2017.

[12] H. Azizpour, A. Sharif Razavian, J. Sullivan, A. Maki, and S. Carlsson, ‘From generic to specific deep representations for visual recognition’, in *Proceedings of the IEEE conference on computer vision and pattern recognition workshops*, 2015, pp. 36–45.

[13] S. S. Yadav and S. M. Jadhav, ‘Deep convolutional neural network based medical image classification for disease diagnosis’, *J. Big data*, vol. 6, no. 1, pp. 1–18, 2019.

[14] S. Xu, H. Wu, and R. Bie, ‘CXNet-m1: anomaly detection on chest X-rays with image-based deep learning’, *IEEE Access*, vol. 7, pp. 4466–4477, 2018.

[15] C. Cong, Y. Kato, H. D. Vasconcellos, J. Lima, and B. Venkatesh, ‘Automated stenosis detection and classification in x-ray angiography using deep neural network’, in *2019 IEEE international conference on bioinformatics and biomedicine (BIBM)*, IEEE, 2019, pp. 1301–1308.

[16] C. Szegedy *et al.*, ‘Going deeper with convolutions’, in *Proceedings of the IEEE conference on computer vision and pattern recognition*, 2015, pp. 1–9.

[17] C.-Y. Fu, W. Liu, A. Ranga, A. Tyagi, and A. C. Berg, ‘Dssd: Deconvolutional single shot detector’, *arXiv Prepr. arXiv1701.06659*, 2017.

[18] H. Zhang, Z. Gao, D. Zhang, W. K. Hau, and H. Zhang, ‘Progressive perception learning for main coronary segmentation in X-ray angiography’, *IEEE Trans. Med. Imaging*, vol. 42, no. 3, pp. 864–879, 2022.

[19] D. Zhang, X. Liu, J. Xia, Z. Gao, H. Zhang, and V. H. C. de Albuquerque, ‘A physics-guided deep learning approach for functional assessment of cardiovascular disease in IoT-based smart health’, *IEEE Internet Things J.*, vol. 10, no. 21, pp. 18505–18516, 2023.

[20] T. Du *et al.*, ‘Training and validation of a deep learning architecture for the automatic analysis of coronary angiography: Automatic recognition of coronary angiography’, *EuroIntervention*, vol. 17, no. 1, p. 32, 2021.